Behavior of control mode switching inverters during transients in sectionalizing distribution networks

Behavior of Control Mode Switching Inverters During Transients in Sectionalizing Distribution Networks

M.H. ROOS*, P.H. NGUYEN*, J. MORREN*⁋ AND J.G. SLOOTWEG*⁋

*: Eindhoven University of Technology, Electrical Engineering, Eindhoven, the Netherlands
⁋: Enexis Netbeheer, Asset Management, 's-Hertogenbosch, the Netherlands
Email: m.h.roos@tue.nl

Abstract:

With the increase of distributed energy resources (DERs) and automated switchgear in distribution networks, sectionalizing distribution networks (SDNs) can be created. Parts of SDNs can be operate in islanded mode when a fault occurs in the network, to continuously supply load with local DERs. Transient stability is a challenge in SDNs due to the fault ride-through, islanding transient and switching between grid-feeding and grid-supporting control modes of DER inverters. To analyze the transient behavior of such control mode switching inverters (CMSIs), a detailed model is created in Simulink and several fault, islanding and control mode switching simulations are performed. The impact of fault clearing time, fault impedance, fault distance, load characteristics, droop constants and grid-feeding power reference values is determined with simulations. From the simulations, the potential problems for the operation of SDNs are identified. Finally, some recommendations for future research are given to improve the transient behavior of CMSIs.

Keywords:

sectionalizing distribution networks, voltage source inverter, transient stability.

1. Introduction

The integration of distributed energy resources (DERs) and automated switchgear into distribution networks enables sectionalizing distribution networks (SDNs). These networks are interconnected during normal operation and can sectionalize the network into islanded microgrids to continue operation when a fault occurs [1]. Autonomous operation of islanded microgrids requires voltage and frequency regulation to be performed by the DERs within the microgrids. During grid-connected operation, DER inverters are operated in grid-feeding mode as current source inverters which cannot provide voltage and frequency regulation. The regulation is usually performed by controlling DER inverters as voltage source inverters in grid-supporting mode [2].

In SDNs, DER inverters have to remain operational during the fault and islanding transients, and switch from grid-feeding to grid-supporting control mode as control mode switching inverters (CMSIs). For grid-supporting mode, droop control is generally used to share active and reactive power between DERs without communication [3]. The microgrids operate autonomously until the fault is cleared, after which the microgrids are resynchronized and reconnected to the main network.

Voltage and frequency deviations outside of the grid code limits can cause disconnection of load and/or generation which may cause a blackout of the network. Therefore the behavior (e.g. output current, voltage) of inverters during fault, islanding and control mode switching transients is critical for effective operation of SDNs.

Preliminary research on behavior of inverters has been mainly focused on small-signal behavior of DERs in grid-connected or isolated microgrids [4]–[6]. However some literature discussed the fault behavior of inverters and indicate that fault clearing time, fault resistance, load characteristics and droop constants impact the transient behavior of inverters [7], [8]. Islanding and control mode switching transients are rarely treated by literature. To fill this research gap, this paper analyzes the behavior of droop-controlled CMSIs during fault, islanding and control mode switching in SDNs. The contributions of this paper are:

1. Analysis of the behavior of CMSIs during fault, islanding and control mode switching transients
2. Identification of possible voltage and frequency violation problems for the operation of SDNs caused by CMSIs
3. Analysis of the impact of fault clearing time, fault resistance, fault distance, grid-feeding power references, load characteristics and droop constants on voltage and frequency.

In the next section a Simulink models of a three-phase two-level inverter and load in a SDN, and the fault, islanding and control mode switching simulations are discussed. The simulation results are discussed in section 3. Finally conclusions and future research directions are given in section 4.

2. Methodology

To perform simulations, a Simulink simulation model of a low voltage (LV) network with a single CMSI is created. Fault, islanding and control mode switching simulations are performed in the network to analyze the transient behavior of CMSIs. A single CMSI is simulated to prevent interactions between CMSIs.

2.1 Inverter

The widely used three-phase two-level inverter with LCL output filter is considered as shown in Fig 1. The primary source of the inverter consists of a 24 V DC voltage source V1 with an internal resistance R1 of 0.0288 Ω representing a 5 kW DER

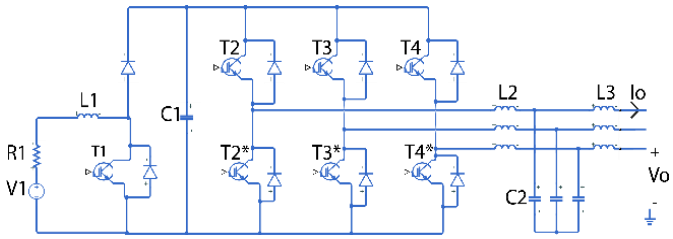

Fig 1. Three-phase two-level inverter with primary source, boost converter, DC-link capacitance and LCL output filter.

such as a battery energy storage system. The primary source supplies a boost converter consisting of inductance L1 of 1 mH, IGBT T1 and two diodes. The boost converter supplies the DC-link and increases the voltage to a minimum of two times the grid voltage. The DC-link voltage is smoothened by capacitance C1 of 10 mF. The inverter consists of six IGBTs (T2, T2*, T3, T3*, T4 and T4*) with antiparallel diodes and is controlled by supplying bipolar PWM pulses at the gates of the IGBTs with a switching frequency of 5 kHz.

The output of the inverter has a high amount of harmonic content which is filtered by a LCL filter. The filter is designed according to the methodology described by [9] with the resonance frequency of 2.5 kHz, a rated reactive power absorption of 5% by capacitor C2, less than 0.1 p.u. filter inductance and current ripple attenuation to 2%. The inductance of L1 and L2 are 13.5 mH and 860 µH respectively, and capacitance C2 is 5 µF with a damping resistance of 12.7 Ω.

2.2 Controllers

As discussed before, CMSIs switch between grid-feeding mode during grid-connected operation and grid-supporting mode during islanded operation. In grid-feeding mode, CMSIs function as current sources to output active and reactive power according to power reference values. The power reference values are the required power output of the DER.

The grid-feeding control structure is shown in Fig 2. The modulation signals for the PWM generator m_d, m_q are generated by two PI controllers which operate in the dq synchronous reference frame. The phase angle of the dq reference frame θ is synchronized with the output voltage of the LCL filter V_o by a phase locked loop (PLL). The reference signals of the PI controllers are determined by dividing the active and reactive power references P^*,Q^* by the d-component of the output voltage V_d. The output current and voltage of the CMSI are limited to 120% of nominal peak values (12.3 A and 390 V) by limiting the PI controllers reference signals.

The controller regulates active (P) and reactive (Q) power output with the modulation signal magnitude and angle according to equations 1a and 1b (for small δ) [10].

$$P \approx \left(\frac{EV_g}{Z} - \frac{V_g^2}{Z}\right)\cos(\theta) + \frac{EV_g}{Z}\delta\sin(\theta) \quad (1a)$$

$$Q \approx \left(\frac{EV_g}{Z} - \frac{V_g^2}{Z}\right)\sin(\theta) - \frac{EV_g}{Z}\delta\cos(\theta) \quad (1b)$$

Where δ is the phase angle between the inverter output

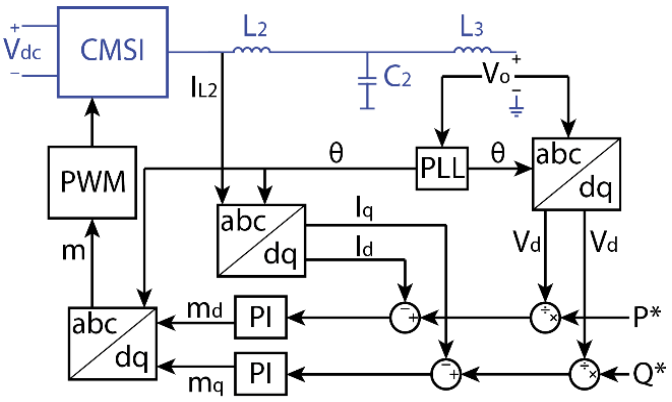

Fig 2. Grid-feeding control structure

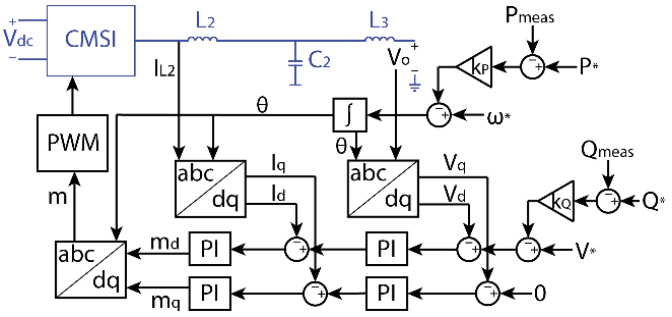

Fig 3. Grid-supporting control structure with conventional droop control

voltage E and the network voltage V_g, and Z and θ are the magnitude and phase of the impedance between E and V_g. In an inductive network, the active and reactive power output are mainly controlled with the phase angle and inverter output voltage magnitude respectively. In a resistive network the active power and reactive power are controlled by the inverter output voltage magnitude and the phase angle respectively. In the dq reference frame, the inverter output voltage magnitude is controlled with the d-component, while the phase angle is controlled with the q-component of the modulation signal.

The PI current controllers are designed with the Matlab function "PIDtune" to increase the controlled current plant bandwidth to 100 times the bandwidth of the uncontrolled plant. The resulting proportional and integral parameters are equal to $P = 0.144$ and $I = 411$ respectively.

The current control of a grid-supporting control structure is similar to the grid-feeding control structure. As shown in Fig 3 the reference values for the current controllers are generated by a set of PI voltage controllers. The reference for the d-component of the voltage is generated by the reactive power droop control, while the q-component reference is set to zero. The frequency and phase angle of the dq reference frame are determined by the active power droop control.

The voltage controllers regulate the output voltage to reference value V^* with zero angle relative to the dq reference frame. In grid-supporting operation with conventional droop control [2], the dq reference frame is synchronized by the active power droop control instead of a PLL. When the measured active power output of the inverter P_{meas} is greater or smaller

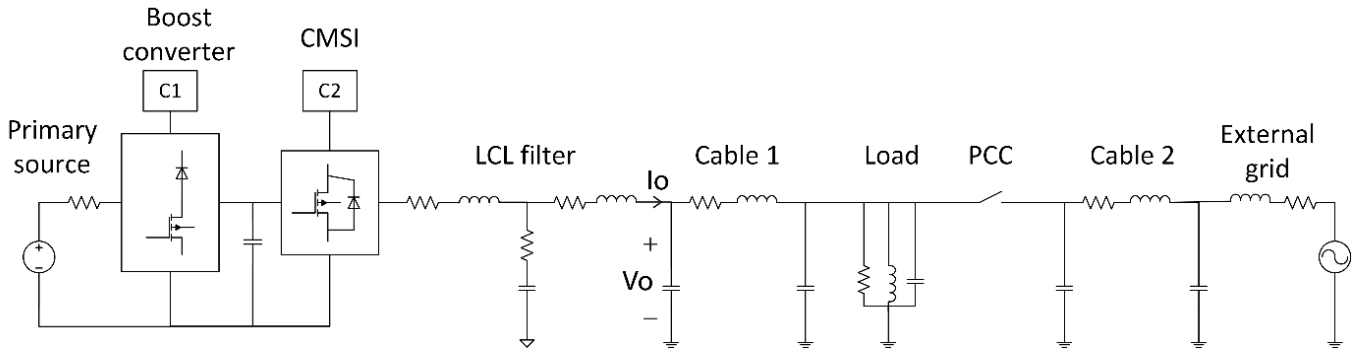

Fig 4. Single line diagram of the simulated network. PS: primary DC source, C1: DC-link voltage controller, C2: inverter controller, V_o: output voltage, I_o: output current.

than the reference power P^*, the frequency should be decreased or increased respectively. The frequency decrease is determined by the power mismatch multiplied with droop constant k_P. When the measured reactive power output of the inverter Q_{meas} differs from the reference power Q^*, the voltage should be changed inversely to the mismatch between Q_{meas} and Q^*.

The cascaded current and voltage controllers are independent by time domain separation. The bandwidth of the controlled current plant is designed to be ten times larger than the bandwidth of the controlled voltage plant. The proportional and integral parameters are equal to $P = 0.0893$ and $I = 537$ respectively. The droop control is designed to output maximum power at 10% voltage deviation and 1 Hz frequency deviation from nominal. The nominal RMS phase voltage is 230 V with a frequency of 50 Hz. Droop constants k_P and k_Q are therefore $\frac{-0.2\pi}{5000}$ and $\frac{-32.5}{5000}$ respectively.

The DC-link voltage of the inverter is dependent on the power generated by the primary source P_{ps}, the power output of the inverter P_o and the losses P_{loss} as described by equation 2 [11]. A PI controller stabilizes the DC-link voltage V_{dc} at the nominal value of 800 V by controlling P_{ps} by adapting the duty cycle of the boost converter.

$$\frac{C}{2}\frac{dV_{dc}^2}{dt} = P_{ps} - P_{loss} - P_o \quad (2)$$

2.3 Network and simulations

The LV network model is developed in Simulink as shown in Fig 4. The CMSI is connected to a load and the point of common connection (PCC) via cable 1. From the PCC, cable 2 connects to the external grid equivalent.

For the inverter and boost converter two Simscape models are used. In the inverter model the individual switching behavior of the IGBTs is modeled for accurate simulation. In the boost converter model the switching behavior is averaged over time to decrease the simulation time. The cables are 4*150 mm^2 aluminum cables with a resistance, inductance and capacitance of 0.206 Ω/km, 0.17 mH/km and 281 µF/km, and are modeled as pi equivalent model. The external grid has a nominal phase voltage of 230 V and a short circuit current capacity of 10 kA. The external grid is modeled as a voltage source in series with a resistance and inductance.

Three types of transient simulations are performed: faults, islanding and control mode switching. Faults are simulated at the terminals of the external grid, islanding is performed by opening the switch at the PCC and control mode switching is performed by switching the controller from grid-feeding to grid-supporting mode. The fault clearing time, fault impedance, load characteristics and droop constants have been identified to impact the transient behavior of inverters. This paper analyzes these properties, as well as the fault distance, and the grid-feeding power references.

2.4 Load

There is a large variety of load types present in distribution networks, usually categorized into residential, commercial and industrial loads. Accurate modeling of loads is important for transient analysis, since the type of load in the network and load models significantly impact the results [12]. The load in the SDN show in Fig 4 is modeled as a single aggregated voltage dependent exponential load. The active and reactive power absorbed by this load models is described by equations 3a and 3b.

$$P_{exp} = P_0\left(\frac{V}{V_0}\right)^{k_{pv}} \quad (3a)$$

$$Q_{exp} = Q_0\left(\frac{V}{V_0}\right)^{k_{qv}} \quad (3a)$$

An exponential load parts has a base power absorption (P_0, Q_0) which are scaled according to the voltage and the load coefficients (k_{pv}, k_{qv}). The load coefficients of the load are selected to be typical for residential loads with non-electric heating [13]: $k_{pv} = 1.5, k_{qv} = 2.5$. The active and reactive power absorption of the load is shown in Fig 6. The active and reactive power absorbed by the load increases when the voltage level increases. In this paper the nominal apparent power of the load (S_{load}) is 2 kVA and the load has a power factor of 0.95, unless specified otherwise.

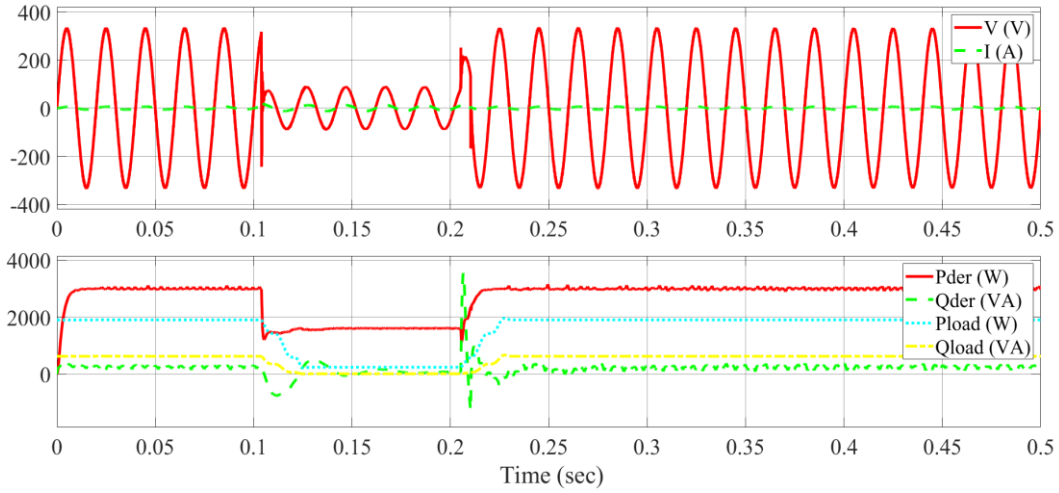

Fig 5. Single phase output voltage (V) and current (I), DER output active power (Pder) and reactive power (Qder), and load active power (Pload) and reactive power (Qload) in case of a 10mΩ three-phase fault at 2.5km for 0.1 seconds.

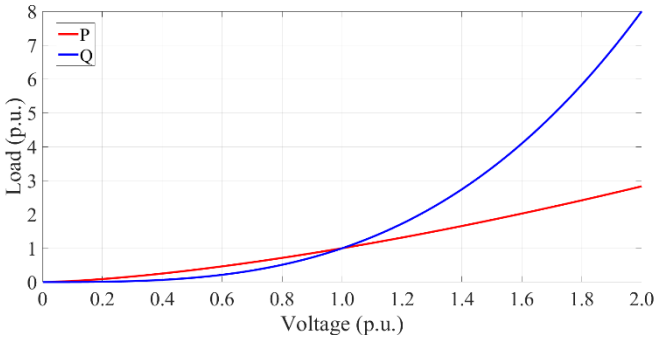

Fig 6.Active (P) and reactive (Q) power absorption of the voltage dependent exponential load at different voltage levels.

3. Results and discussion

3.1 Steady-state grid-connected operation

The grid-feeding control structure accurately tracks the power reference values in grid-connected operation. With P^* = 3 kW and Q^* = 0 kVA the voltage magnitude is near nominal with a frequency of 50 Hz, and the active and reactive power outputs are 3 kW and 0 kVA. Since the load absorbs an apparent power of 2 kVA, the remaining part of the active power generated by the DER is fed into the external grid.

3.2 Faults

The output voltage, current, active power and reactive power during a three-phase fault with a fault impedance of 10 mΩ for 0.1 seconds at the terminals of the external grid are shown in Fig 6. The output current and voltage at the CMSI terminals for different fault impedance and cable length are shown in table I. The external grid is located 2.5 km from the inverter where cable 1 and 2 are 2 km and 0.5 km long respectively. The output current I_o of the inverter increases from 5 A to the limited value of 8.7 A with a peak of 18 A at the fault instant. Although the output current increases, the low impedance causes the output voltage V_o to decrease to 63 V. A single-phase to earth fault produces similar results, however the voltage and current changes occur on a single phase. The active power output P_o decreases to 1.5 kW during the fault and returns to the reference value after the fault is cleared.

TABLE I
CMSI OUTPUT VOLTAGE AND CURRENT DURING FAULTS WITH DIFFERENT FAULT IMPEDANCE AND CABLE LENGTH

Property	Quantity	Output voltage (V)	Output current (A)
Fault impedance (mΩ)	1	11	8.7
	10	63	8.7
	100	187	5.5
Fault distance (km)	2.5	63	8.7
	5	64	8.7
	10	72	8.7

The fault impedance has a significant impact on the output voltage and current during a three-phase fault as shown in table I. With a fault impedance of 1 mΩ the output voltage decreases to 11 V, while the current is limited at 8.7 A. Therefore the output power decreases to less than 300 W during the fault. With a high fault impedance of 100 mΩ the voltage remains decreases significantly less and the output current in less than the limited value.

The fault distance has a smaller impact on the voltage and output current during the fault. A larger fault distance reduces the effect of a fault as shown in table I. When a three-phase fault occurs at 10 km distance (cable 1 and 2 are 2 km and 8 km long respectively), the voltage decreases to 72 V while the output power decreases to approximately 1.9 kW.

The fault clearing time has no significant effect on the behavior of the CMSI besides the duration of the fault period.

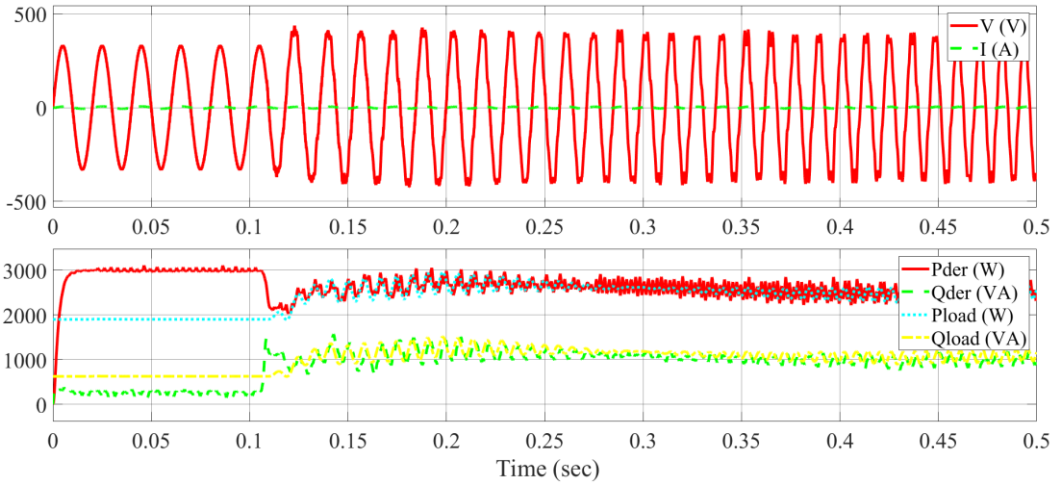

Fig 7. Single phase output voltage (V) and current (I), DER output active power (Pder) and reactive power (Qder), and load active power (Pload) and reactive power (Qload) in case of islanding at 0.104 seconds with a load power factor of 0.95.

3.3 Islanding

TABLE II
CMSI OUTPUT VOLTAGE AND VOLTAGE FREQUENCY DURING ISLANDING WITH DIFFERENT GRID-FEEDING POWER REFERENCES AND LOAD POWER FACTORS

Property	Quantity	Output voltage (V)	Frequency (Hz)
Active power reference (kW)	1.5	205	68
	3	283	89
	5	283	93
Load power factor	1	276	27
	0.95	283	89
	$\sqrt{0.5}$	290	175

The output voltage, current, active power and reactive power during islanding with a balanced exponential load are shown in Fig 7. The output voltage of the CMSI and voltage frequency in the network for different grid-feeding active power references and load power factors is shown in table II. When the network is islanded, the voltage increases to 283 V while the current decreases to 3.5 A. At a voltage of 283 V the load active power is equal to 2.6 kW. The frequency in the islanded network increases to 89 Hz after 0.4 seconds of islanding.

The grid-feeding control power references before islanding greatly impact the voltage, current and frequency when islanding. When the active power reference is 1.5 kW, the voltage decreases to 205 V while the current increases from 2.4 A to 2.8 A during islanding as shown in table II. During 0.4 sec of islanding, the frequency increases to 68 Hz.

The power factor of the load has a significant impact on the voltage frequency in the network during islanding in grid-feeding CMSI operation. When the load inductive with a power factor of $\sqrt{0.5}$, the frequency increases to 175 Hz after 0.4 seconds of islanding which is significantly higher than the frequency with a power factor of 0.95. With a purely resistive load the frequency in the network decreases to 27 Hz after 0.4 seconds of islanding.

3.4 Control mode switching

When switching from grid-feeding to grid-supporting operation, the output voltage and frequency change according to droop the droop constants while the output power changes to the load value. With a load of 2 kVA and a power factor of 0.95, the output voltage is 228 V which the frequency changes to 48 Hz as shown in Fig 8 and table III. During the islanded operation the voltage and frequency deviation from nominal are significant, however after switching to grid-supporting operation the voltage and frequency are near nominal values.

The load power factor slightly impacts the steady-state voltage and frequency after control mode switching. With an inductive load the voltage deviation from nominal is larger than with a resistive load, while the frequency deviation is larger with a resistive load. Changing the droop constants has limited impact on the transient behavior of the CMSI. A smaller droop constant improves tracking of the nominal voltage and frequency.

3.5 Combined

When sequentially simulating a fault, islanding and control mode switching transients, the operation of a SDN is replicated. The combined simulation with a 1 mΩ three-phase fault, a 2kVA load with power factor of $\sqrt{0.5}$, and 1.5 kW active power reference is shown in Fig 9. When a fault occurs the voltage waveform becomes highly distorted with an RMS value of 11 V, the current increases to the limited value of 8.7 A, and the active power decreases to less than 300 W. During islanded operation, the voltage increases to 320 V, while the active and reactive power output increases to around 2 kW and 2.5 kVA respectively. After switching to grid-supporting mode, the voltage changes to 228 V with a frequency of 48 Hz. The active and reactive power output of the CMSI with grid-supporting

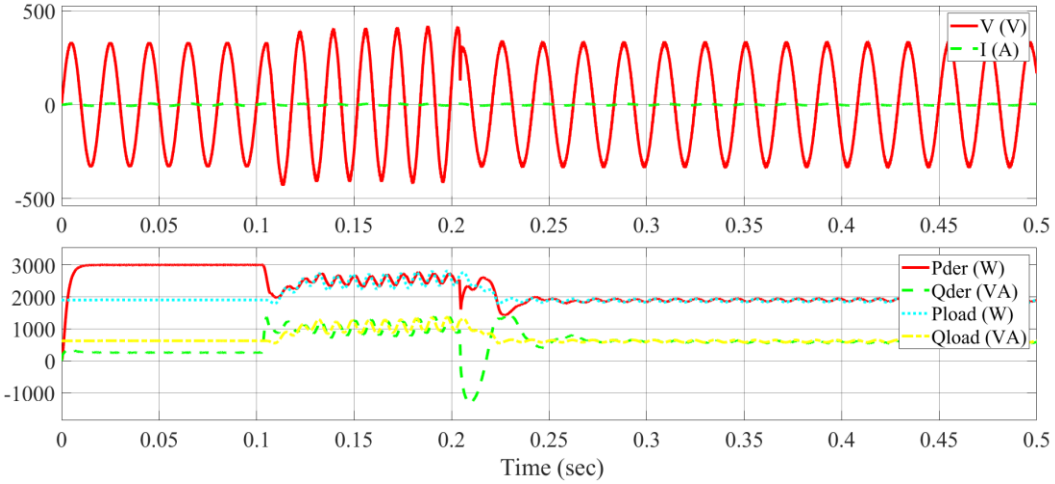

Fig 8. Single phase output voltage (V) and current (I), DER output active power (Pder) and reactive power (Qder), and load active power (Pload) and reactive power (Qload) in case of islanding at 0.104 seconds and control mode switching at 0.204 seconds. The load power factor is 0.95 and the droop constants are $\frac{-0.2\pi}{5000}$ and $\frac{-32.5}{5000}$.

control are equal to the active and reactive power demanded by the load.

3.6 Discussion

The behavior of a CMSI, network voltage and frequency during fault, islanding and control mode switching transients is analyzed using a Simulink model of a network with a single CMSI and load connected to an external grid equivalent. The transients are analyzed individually and sequentially to replicate the behavior in a SDN.

The transient simulations showed that large voltage and frequency deviations from nominal occur during faults and islanding with grid-feeding control. The voltage and frequency deviation can damage components and cause disconnection of generation and load in the network. Disconnection of generation and load when part of the network switches to islanded mode can complicate balancing generation and demand within the network. This threatens the operation of SNDs after switching to islanded mode. Disconnection of load also counteracts the objective of SDNs, which is to supply load after a fault occurs.

The disconnection behavior of load and DER due to voltage and frequency deviations was not included in models in this paper. The load and DER with CMSI are assumed to remain operational while severe voltage and frequency deviations occur. During all simulated faults the voltage is lower than the default fault ride-through settings described by the IEEE 1547-2018 standard which requires DERs with default settings to disconnect from the network [14]. Residential load usually has a cut-off voltage of around 0.5 p.u. which causes the load to switch off during the faults [15]. During islanded operation with mixed or dominantly inductive load the frequency violates the European grid code which allows DERs to disconnected from the network [16]. Due to the short duration of the voltage and frequency violations, it is unclear if the DER and load remain operational in practice.

Control mode switching does not cause any violations in the simulations and changes the voltage and frequency in the network to near-nominal values according to the droop characteristics. However in a network with multiple CMSIs, the interaction between droop-controlled CMSIs may cause stability problems as described by [4].

TABLE III
CMSI OUTPUT VOLTAGE AND VOLTAGE FREQUENCY AFTER CONTROL MODE SWITCHING WITH DIFFERENT LOAD POWER FACTORS AND DROOP CONSTANTS

Property	Quantity	Output voltage (V)	Frequency (Hz)
Load power factor	1	230	48
	0.95	228	48
	$\sqrt{0.5}$	226	49
Droop constants	$\frac{-0.4\pi}{5000}, \frac{-65}{5000}$	226	46
	$\frac{-0.2\pi}{5000}, \frac{-32.5}{5000}$	228	48
	$\frac{-0.02\pi}{5000}, \frac{-3.25}{5000}$	230	50

The transient behavior of CMSIs can be improved by modifying the droop controllers e.g. with virtual impedance droop control [7]. Alternatives are the addition of a secondary controller which adapts the active and reactive power references of the droop controller or the replacement of the droop controller by an active power sharing controller [17]. The addition of reactive power compensators such as STATCOMs can also improve the transient performance by changing the voltage to nominal value by reactive power injection [7].

4. Conclusion and future research

When a fault occurs in SDNs supplied by CMSIs, the network attempts to continue operation by islanding part of the network. However, during a fault, transition to islanded operation and islanding with grid-feeding control the voltage and frequency deviates significantly from nominal. These deviations can cause disconnection of generation and load in the network preventing continuous operation of SDNs. The voltage

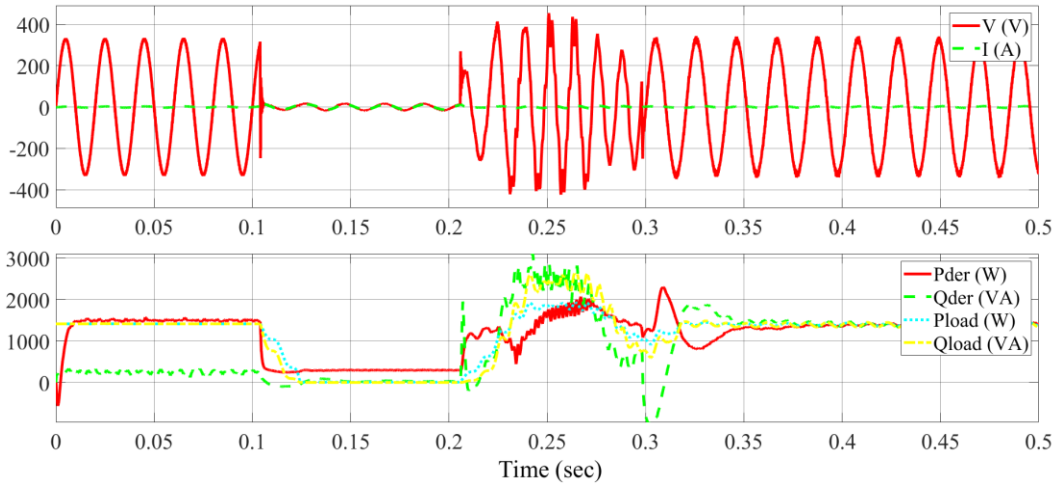

Fig 9. Single phase output voltage (V) and current (I), DER output active power (Pder) and reactive power (Qder), and load active power (Pload) and reactive power (Qload) in case of a fault at 0.104 seconds, islanding at 0.204 seconds and control mode switching at 0.304 seconds.

and frequency deviation mainly depends on the fault impedance, load type and grid-feeding power references. The droop constants have no significant impact on the transient behavior of a single CMSI.

The interaction between multiple droop-controlled CMSIs, the disconnection behavior of load and DERs during large voltage and frequency deviations, improving the transient behavior with alternative controllers, and resynchronization and reconnection after faults are cleared are going to be treated by the authors in future research. The impact of the PLL of CMSIs on the changing frequency during islanding in grid-feeding operation should also be researched.

References

[1] Z. Wang and J. Wang, "Self-healing Resilient Distribution Systems based on Sectionalization into Microgrids," *IEEE Trans. Power Syst.*, vol. 30, no. 6, pp. 3139–3149, 2015.

[2] J. Rocabert, A. Luna, F. Blaabjerg, and I. Paper, "Control of Power Converters in AC Microgrids," *IEEE Trans. Power Electron.*, vol. 27, no. 11, pp. 4734–4749, 2012.

[3] D. E. Olivares, A. Mehrizi-Sani, A. H. Etemadi, C. A. Cañizares, R. Iravani, M. Kazerani, A. H. Hajimiragha, O. Gomis-Bellmunt, M. Saeedifard, R. Palma-Behnke, G. A. Jiménez-Estévez, and N. D. Hatziargyriou, "Trends in microgrid control," *IEEE Trans. Smart Grid*, vol. 5, no. 4, pp. 1905–1919, 2014.

[4] X. S. Tang, X. Hu, N. N. Li, W. Deng, and G. W. Zhang, "A Novel Frequency and Voltage Control Method for Islanded Microgrid Based on Multienergy Storages," *IEEE Trans. Smart Grid*, vol. 7, no. 1, pp. 410–419, 2016.

[5] X. Tang, W. Deng, and Z. Qi, "Investigation of the dynamic stability of microgrid," *IEEE Trans. Power Syst.*, vol. 29, no. 2, pp. 698–706, 2014.

[6] N. Bottrell, M. Prodanovic, and T. C. Green, "Dynamic stability of a microgrid with an active load," *IEEE Trans. Power Electron.*, vol. 28, no. 11, pp. 5107–5119, 2013.

[7] Z. Shuai, Y. Sun, Z. J. Shen, W. Tian, C. Tu, Y. Li, and X. Yin, "Microgrid stability: Classification and a review," *Renew. Sustain. Energy Rev.*, vol. 58, pp. 167–179, 2016.

[8] A. H. Kasem Alaboudy, H. H. Zeineldin, and J. Kirtley, "Microgrid stability characterization subsequent to fault-triggered islanding incidents," *IEEE Trans. Power Deliv.*, vol. 27, no. 2, pp. 658–669, 2012.

[9] M. Liserre, F. Blaabjerg, and S. Hansen, "Design and control of an LCL-filter-based three-phase active rectifier," *IEEE Trans. Ind. Appl.*, vol. 41, no. 5, pp. 1281–1291, 2005.

[10] Q. C. Zhong and Y. Zeng, "Universal Droop Control of Inverters with Different Types of Output Impedance," *IEEE Access*, vol. 4, pp. 702–712, 2016.

[11] A. Yazdani and R. Iravani, *Voltage-Sourced Converters in Power Systems*. Hoboken, NJ, USA: John Wiley & Sons, Inc., 2010.

[12] IEEE Task Force on Load Representation for Dynamic Performance, "Load representation for dynamic performance analysis," *IEEE Trans. Power Syst.*, vol. 8, no. 2, pp. 472–482, 1993.

[13] L. M. Korunović, S. Member, J. V Milanović, S. Ž. Djokić, K. Yamashita, S. M. Villanueva, S. Sterpu, and S. Member, "Recommended Parameter Values and Ranges of Most Frequently Used Static Load Models," vol. 8950, no. c, pp. 1–12, 2018.

[14] IEEE standards association, *IEEE Standard for Interconnection and Interoperability of Distributed Energy Resources with Associated Electric Power Systems Interfaces Sponsored by the IEEE Standard for Interconnection and Interoperability of Distributed Energy Resources with Associate*. 2018.

[15] A. Bokhari, A. Alkan, R. Dogan, M. Diaz-Aguilo, F. De

Leon, D. Czarkowski, Z. Zabar, L. Birenbaum, A. Noel, and R. E. Uosef, "Experimental determination of the ZIP coefficients for modern residential, commercial, and industrial loads," *IEEE Trans. Power Deliv.*, vol. 29, no. 3, pp. 1372–1381, 2014.

[16] European commission;, "Commission Regulation (Eu) 2016/631 Establishing a Network Code on Requirements for Grid Connection of Generators," *Off. J. Eur. Union*, no. 14 April 2016, p. 68, 2016.

[17] X. Han, K. Heussen, O. Gehrke, H. W. Bindner, and B. Kroposki, "Taxonomy for Evaluation of Distributed Control Strategies for Distributed Energy Resources," *IEEE Trans. Smart Grid*, vol. 3053, no. c, pp. 1–1, 2017.

M.H. (Martijn) Roos (S'18) received the B.Eng. degree in electrical engineering from HAN University of Applied Sciences, Arnhem, the Netherlands in 2014 and the M.Sc. degree in electrical engineering from Eindhoven University of Technology, Eindhoven, the Netherlands in 2017 (cum laude), where he is currently working towards the Ph.D. degree in the field of control and protection of sectionalizing distribution networks at the Electrical Energy Systems group. His main research interests include operation of microgrids during transients, real-time control of distributed energy resources, adaptive protection systems, modeling of distributed energy resources and loads, and smart grids.

P.H. (Phuong) Nguyen (M'06) was born in Hanoi, Vietnam, in 1980. He is assistant professor of Electrical Energy Systems group at the Eindhoven University of Technology, the Netherlands. He received the B.E. degree in electrical engineering at Hanoi University of Technology, Vietnam, in 2002 and the M.Eng. degree in the electrical engineering department, at the Asian Institute of Technology, Thailand, in 2004. In 2010, he received his Ph.D. at the Eindhoven University of Technology, the Netherlands, and was employed at the same group as a postdoctoral researcher. He has been a visiting researcher with the Real-Time Power and Intelligent Systems (RTPIS) Laboratory, Clemson University, US in 2012 and 2013. His research interests include distributed state estimation, control and operation of the power system, multi-agent system, and their applications in the future power delivery system.

J. (Johan) Morren (M '03) received the M. Sc. and Ph.D degree in Electrical Power Engineering both from the Delft University of Technology, The Netherlands in 2000 and 2006 respectively. Since 2006 Johan is consultant with the Asset Management department of Enexis B.V., one of the largest Distribution Grid Operators of the Netherlands. His main areas of interest are protection, automation and control, distributed generation and switchgear. He is also assistant professor (part-time) at the Electrical Energy Systems group at the Eindhoven University of Technology, the Netherlands.

J.G. (Han) Slootweg (M'00) received the M.Sc. degree in electrical power engineering in 1998 (cum laude) and the Ph.D. degree in 2003, both from Delft University of Technology, Delft, The Netherlands. He also received the M.Sc. degree in business administration. He is currently Director of the Asset Management Department of Enexis Netbeheer B.V., Hertogenbosch, The Netherlands, one of the largest Distribution Network Operators of the Netherlands. Its spearheads are the strategic goals of Enexis: accelerating the transition towards a more sustainable energy supply and excellent, state of the art network operation. Han also holds a professorship in Smart Grids at the Electrical Energy Systems group at the Eindhoven University of Technology. He has (co-)authored more than 200 papers, covering a broad range of various aspects of electrical power systems.